

# Monte Carlo simulation of the microPET FOCUS system for small rodents imaging applications

S. Jan<sup>1</sup>, A. Desbrée<sup>2</sup>, F. Pain<sup>2</sup>, D. Guez<sup>3</sup>, C. Comtat<sup>1</sup>, H. Gurden<sup>2</sup>, S. Kerhoas<sup>3</sup>, P. Lanière<sup>2</sup>, F. Lefebvre<sup>2</sup>, R. Mastroiolo<sup>2</sup>, R. Trebossen<sup>1</sup>

<sup>1</sup>Service Hospitalier Frédéric Joliot, CEA/DSV/DRM, Orsay, France

<sup>2</sup>Institut de Physique Nucléaire, CNRS/IN2P3, Orsay, France

<sup>3</sup>SPhN, CEA/DSM/DAPNIA, Saclay, France

## I. INTRODUCTION

Positron Emission Tomography is an essential tool for small animal imaging and more generally for molecular imaging. Growing requirements in velocity and precision imply the optimization of acquisition parameters and protocols. Monte Carlo simulations are essential tools for assisting these developments, improving data analysis and image quantification. In this work we use the GATE platform [1] based on the Geant4 toolkit package and dedicated to nuclear medicine imaging. GATE is well suited for modelling the microPET FOCUS system dedicated to small animal PET imaging and for implementing a realistic voxelized rat brain phantom. In this paper, we compare the performances of the simulator against the microPET FOCUS scanner in order to validate the use of the model for quantitative analysis and simulations of realistic rat brain exams are performed. In a preliminary study, we show how the corrections of physical effects such as positron range and  $\gamma$  acollinearity can reduce the bias on the rat brain quantitative analysis using C-11 or F-18 as radioisotopes.

## II. MATERIAL AND METHODS

### A. The microPET FOCUS system

The microPET FOCUS is the last generation of commercial PET scanners dedicated to small animal imaging such as the rodents (mice and rats) and the primates (macaque or small baboon). The main characteristics of the microPET FOCUS system are:

- Radial Field of View (FOV): 24.2 cm
- Axial FOV: 7.6 cm
- Volume resolution at center of FOV: 2.5  $\mu$ l
- Absolute sensitivity at center of FOV: 3.4 %

The microPET FOCUS system uses an LSO block: 12x12 array of crystals of 1.5x1.5x10 mm<sup>3</sup> each. 168 blocks are arranged in 4 axial rings.

### B. GATE: the Monte Carlo platform

GATE encapsulates the Geant4 libraries to achieve a modular, versatile and scripted simulation toolkit adapted to emission and transmission tomography. It allows describing time-dependent phenomena such as detector or patient movements, source decay kinetics, time window for coincidence acquisitions. Two sets of simulations were compared to experimental data: spatial resolution measurements and counting rate for prompt and delay

coincidences. For the image resolution estimation, radial and tangential FWHM were measured with a <sup>18</sup>F point sources embedded in a capillary tube (0.2 mm internal diameter) and placed at different locations in the radial FOV. To validate GATE on the spatial resolution measurement, we simulated the explicit emission of the positrons by taking into account their

range and the acollinearity of the annihilation photons. A Gaussian blurring function is applied to the detection position of the photon within the crystal to mimic resolution degradation induced by crystal scintillation and light collection. To measure the counting rate performances, a 34 ml and 3 cm diameter cylindrical phantom was used. The phantom was uniformly filled with a C-11 aqueous source with an initial activity of 12 mCi. Some dedicated modules were developed and incorporated within GATE to simulate the complete electronic dead time chain and the delay coincidences measurements [2]. The energy window was set to 350-750 keV and the coincidence time window to 6 ns. All images were reconstructed with an OSEM2D algorithm after a Fourier Rebinning (FORE).

### C. The voxelized rat brain phantom

The voxelized rat brain phantom used in this study (Figure 1), is based on Paxinos and Watson's rat brain atlas in stereotaxic coordinates [3] which describes in 78 coronal slices the brain structures delineations for an average 290g male Wistar rat. These digital slices have been manually segmented in 16 regions of interests including Cerebellum, Ventricles, Aqueduct, dopaminergic structures such as the Caudate Putamen, the Globus Pallidus, the Nucleus accumbens, the Substantia Nigra; and serotonergic structures such as the Dorsal Raphe Nucleus and the Hippocampus. Since the initial slices from Paxinos and Watson were not equidistant, linear interpolation has been carried out to produce 107 coronal segmented slices each separated by 200  $\mu$ m. The final phantom consists of a 54x78x107 matrix composed of 200  $\mu$ m side cubic voxels.

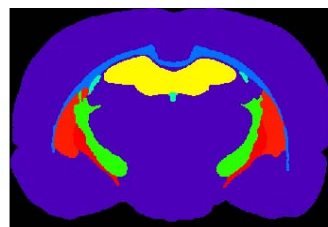
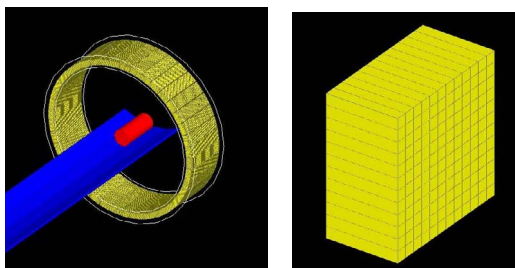


Figure 1: A transaxial slice of the numerical rat brain atlas.

### III. RESULTS

#### A. Validations for the microPET FOCUS simulation

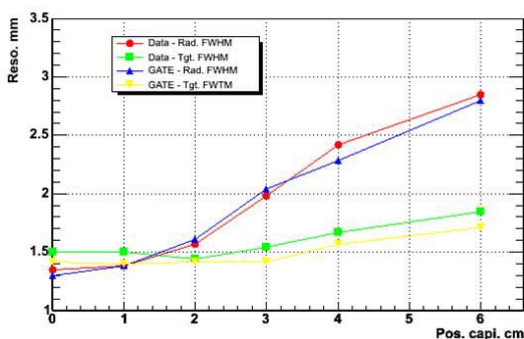
As illustration, a description of the microPET FOCUS by GATE is shown in Figure 2: the full acquisition setup for counting rate measurements and quantification validation with the carbon bed and the cylindrical phantom (left), the complete description of LSO block with 144 crystals (right).



**Figure 2:** microPET FOCUS geometry performed by GATE.

##### 1. Spatial resolution

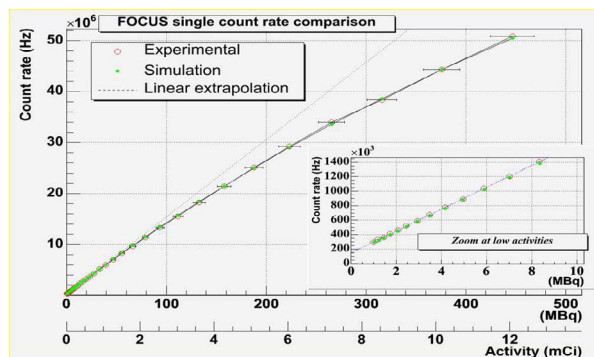
The spatial resolution was measured using a glass capillary filled with F-18 aqueous source. Figure 3 shows the differences between GATE simulations and experimental data for radial and tangential resolutions. The discrepancy is lower than 3 %.



**Figure 3:** Evaluation of the spatial resolution (FWHM) with GATE compared with experimental values.

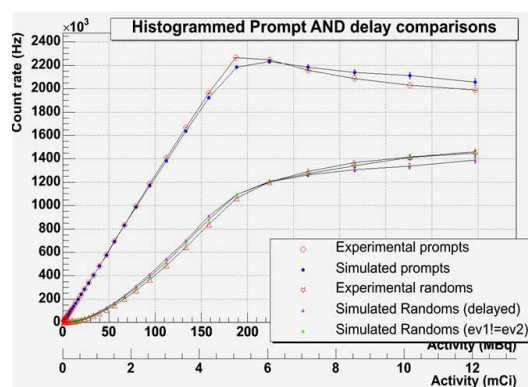
##### 2. Counting rate

A comparison between simulated and experimental data for single count rate is shown in Figure 4. To simulate the physical background noise and the dead time of each block detector, two specific modules were included in the digitizer chain [2]. The results from simulations and measurements are in agreement for a large range of activity in the field of view (from 0 to 12 mCi).



**Figure 4:** Evaluation of the counting rate of the microPET FOCUS with GATE compared with experimental values.

In the lower right side of the Figure 4, the data are plotted for the lowest activities to demonstrate the influence of the physical background digitizer module without any activity in the field of view.



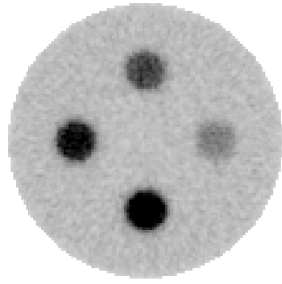
**Figure 5:** Evaluation of the counting rate of the microPET FOCUS with GATE compared with experimental values.

Figure 5 illustrates the comparison between simulated and experimental data for prompt and delay coincidences. The dead time of the coincidence processor and the data transfer from the scanner to the hard disk are also simulated with two specific digitizer modules [2]. As for single counting rate, these results show a very good agreement for a large range of activity in the field of view.

##### 3. Contrast recovering

A 7 cm diameter cylinder with four 1 cm diameter inserts was simulated to measure the contrast recovering. The activity ratios simulated between inserts and the background are 2:1, 3:1, 4:1 and 5:1 respectively for the rod1, rod2, rod3 and rod4.

Figure 5 shows the result after full simulation and reconstruction of this phantom. The contrast recovery results for each insert are listed in table 1.



**Figure 5:** Full simulation and reconstruction of a cylindrical phantom with hot inserts for contrast imaging measurement.

Contrast recovery Rod 1	96 % $\pm$ 3 %
Contrast recovery Rod 2	94.6 % $\pm$ 3 %
Contrast recovery Rod 3	93.7 % $\pm$ 3 %

**Table 1:** Contrast recovery results for each rod. The activity ratio with the background is 2:1 for the rod1, 3:1 for the rod2, 4:1 for the rod3 and 5:1 for the rod4.

#### 4. Quantitative and dynamic imaging

To evaluate the potentiality to simulate a dynamic acquisition with a quantitative analysis, we performed a simulation with the previous 34 ml cylinder phantom filled with 1 mCi of C-11 and with 10 minutes acquisition time. Twenty billions of particles were generated on a cluster and the computing time was close to 4 hours. Figure 6 illustrates a dynamic reconstruction where 6 frames were reconstructed with the following framing: 10 sec, 20 sec, 30 sec, 60 sec, 180 sec and 300 sec.

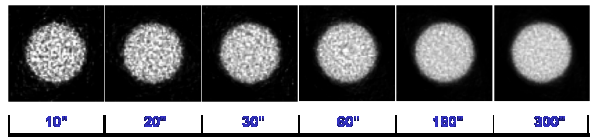


**Figure 6:** Multi-framing reconstruction for dynamic acquisition.

On the figure 7, we compare the quantitative results in Bq/cc between the 6 frames and the theoretical activity included in the phantom. A non-perfect linearity and a discrepancy on the absolute quantitative values can be observed. These two phenomena can be explained by the non-optimized delay and dead-time corrections in our simulated data analysis and also by a non exact normalization during the reconstruction. Finally, the activity reconstructed and the quantitative analysis are over estimated by 7 to 11 %.

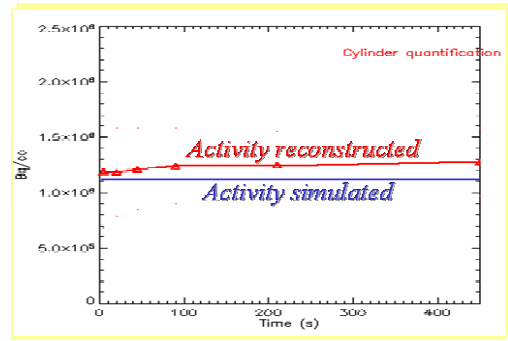


**Figure 7:** Quantification results after the full simulation and reconstruction.

#### 5. Phantom implementation and cluster computing

The voxelized rat brain phantom is used in GATE as an emission map to distribute the activity in the different 15 structures and as an attenuation map to mimic the brain tissue absorption. The complete simulation platform was installed on a cluster of 512 CPU's with a 64 bits architectures and a Linux operating system. This specific configuration was used in order to generate a realistic acquisition of rat brain exams.

##### B. Application for rat brain imaging

###### 1. Preliminary simulation for [F-18]FDG exam

We simulated an activity map close to the rat brain FDG distribution at late acquisition time for a classical exam. Figure 8 shows preliminary results after a full simulation for  $267.10^6$  particles generated in 6 of the 15 brain structures (putamen, cerebellum, globus pallidus, hippocampus and colliculus).

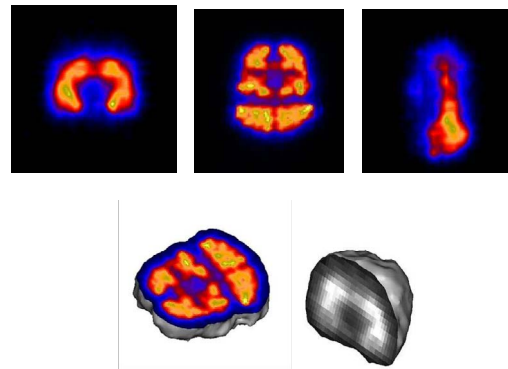


**Figure 8:** Reconstructed images of 6 rat brain structures with an activity map close to the FDG distribution. Transaxial, coronal, sagittal slices and 3D mapping.

###### 2. Preliminary simulation for [C-11]Raclopride exam

The complete rat brain atlas, with the 15 structures, was used in this study to simulate a realistic [C-11]Raclopride exam. The activity map introduced in the phantom was similar to the realistic distribution a late acquisition time. We simulated 750  $\mu$ Ci in the brain for 15 minutes

acquisition time. Figure 9 illustrates results for transaxial, coronal and sagittal slices (top images). The qualitative results from simulation and experiments are quite similar. From a quantitative point of view, the activity ratios between putamen and cerebellum are close to 2:1 for simulation and experimental data. We note that Harderian glands and rat body are not simulated.

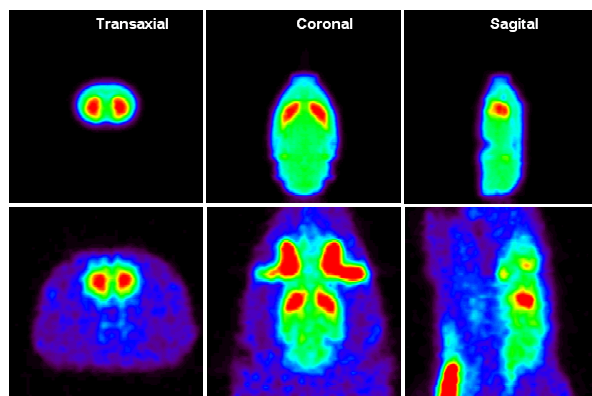


**Figure 10:** Top: Simulation of the full rat brain phantom with an activity map close to the Raclopride distribution – Bottom: Real [C-11]Raclopride rat brain exam with the microPET FOCUS system.

### 3. A quantitative study: physical parameters effects on the quantification

The activity distribution was included in 4 structures of the rat brain: the Caudate Putamen, the Globus Pallidus, the Hippocampus and the Colliculus. We perform 2 sets of simulation, one with a direct gamma/gamma emission and the other one with the C-11 decay to include the positron range and gamma acolinearity effects. Figure 11 and figure 12 show the impact of these 2 effects on the image resolution.

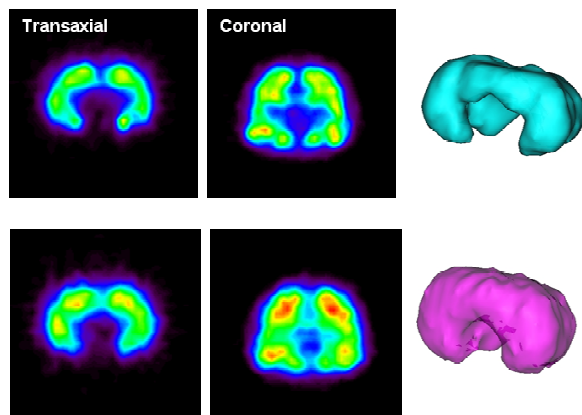


**Figure 11:** Top: Transaxial, coronal slices and 3D mapping reconstructed for 4 rat brain structures simulated with a gamma/gamma emission – Bottom: Transaxial, coronal slices and 3D mapping reconstructed for 4 rat brain structures simulated with a C-11.

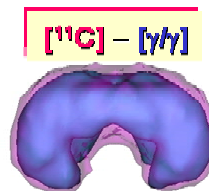


**Figure 12:** 3D mapping of the 4 rat brain structures for gamma/gamma simulation (blue) includes in the C-11 simulation (magenta).

To evaluate the consequences of these physical effects on the sensitivity and the quantitative analysis, we defined a region of interest (ROI) on the Caudate Putamen structure (Figure 6 - left) and we compared the activity value for F-18, C-11 and pure gamma/gamma emission (to mimic a full correction of positron range and gamma acolinearity). Figure 6 (right) shows that the bias on the quantification in the caudate putamen structure can be reduced by 30% for C-11 and 25% for F-18 if corrections of physical effects are taken into account.

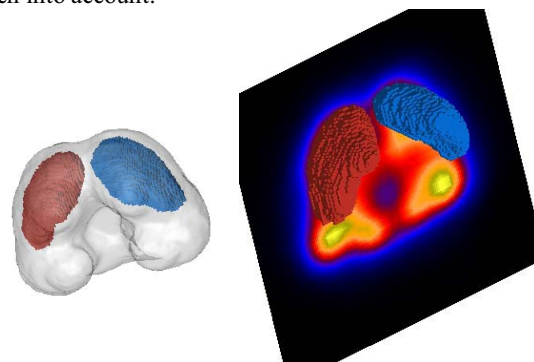


**Figure 13:** Left: Determination of the ROI on the caudate putamen for the gamma/gamma simulation – Right: Fusion of the previous ROI on the C-11 simulation.

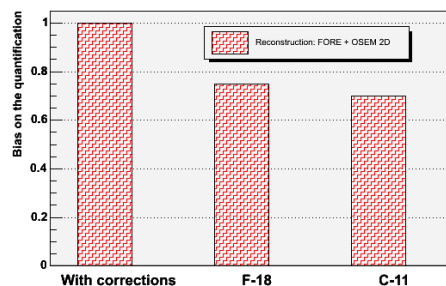


**Figure 14:** Bias on the quantification induced by the positron range and gamma acolinearity.

## IV. CONCLUSION & PERSPECTIVES

In this paper we validated the microPET FOCUS modelling with GATE. We presented the performances of this Monte Carlo platform on voxelized rat brain phantom, specially for the simulation of realistic [C-11]Raclopride exam with a realistic modelling of the injected dose and acquisition time. These results are the consequence of the complete installation of this Monte Carlo platform simulation on a cluster computing architecture. Finally, we showed a first preliminary approach to improve the quantitative analysis in rat brain dopaminergic studies with

an implementation of corrections about the positron range and  $\gamma$  acolinearity effects.

In the future, these corrections could be included as priors in a Maximum *a posteriori* ( MAP [4]) reconstruction algorithm.

Moreover, the simulation of whole body exams can be planned in order to optimize the quantitative analysis for small animal PET imaging.

## References

- [1] Jan S *et al* "GATE: a simulation toolkit for PET and SPECT", Phys. Med. Biol. 49 (2004) 4543-4561.
- [2] Guez D. et al. "Counting rates and dead time modelisations for PET scanners with GATE" to be submitted in IEEE TNS.
- [3] Paxinos G, Watson C (1998) The rat stereotaxic coordinates, 4th Edition. San Diego: Academic Press.
- [4] Qi J *et al*. "High-resolution 3D Bayesian image reconstruction using the microPET small animal scanner", Phys. Med. Biol. 43 (1998) 1001-1013.